## PAPER

Check for updates

# The impact of aggregation of AIE and ACQ moiety-integrating material on the excited state dynamics †

Gui-Yuan Wu, [ID] *[a] Hui-Min Zhu,[a] Hao Li,[a] Kai Zhang, [ID] [b] Xianyi Zhang,[a] Dong Yan, [ID] [c] Xiu-Du Zhang,[c] Lili Lin [ID] *[b] and Zhou Lu [ID] *[a]

The investigation of the properties of aggregate materials is highly interesting because the process of aggregation can result in the disappearance of original properties and the emergence of new ones. Here, a novel fluorescent material (**TPEIP**), which synergistically combines aggregation-induced emission (AIE) and aggregation caused quenching (ACQ) moieties, was first synthesized by the cyclization reaction of 2,3-diamino-phenazine with 4-tetraphenylenthenealdehyde. We controlled the degree of aggregation of **TPEIP** to shed light on the impact of the aggregation on the excited state dynamics. **TPEIP** aggregation realized control over the Intersystem Crossing (ISC) rates and, in turn, the suppression of triplet excited states in MeOH, EtOH or *via* the simple addition of water to **TPEIP** solutions in DMSO. From global target analysis, the time scale was 966.2 ps for ISC for **TPEIP** in DMSO, but it was 860 ps in the case of **TPEIP** solutions featuring 5% water. The dynamics of **TPEIP** excited states undergo significant changes as the degree of aggregation increases. Notably, the lifetime of singlet excited states decreases, and there was a gradual diminishment in triplet states.

## Introduction

Aggregates have been a prominent research topic in the field of self-assembly, playing an indispensable role in the domains of biology, chemistry, and materials science.[1] Specifically, aggregates are entities composed of two or more interacting components at the mesoscale, with normal dimensions ranging from nanometers to millimeters, bridging the large gap between microscopic molecules and macroscopic matter. There is plenty of room in the middle to explore and unlock the mysteries of the middle world.[2] Therefore, "aggregate science" deserves more attention and exploration in its own right rather than being considered merely an "extension package" of molecular science programs. Although properties always depend on the structure–property relationship, the term "structure" no longer solely refers to the molecular chemical structure but also encompasses the mesoscopic structure of aggregates.[3] Therefore, the elucidation of the relationship between aggregates and properties is imperative for the construction of novel organic compounds and the advancement of multifunctional materials.

In materials science, research beyond molecules attracts more and more attention, as represented by research in molecular self-assembly, supramolecular chemistry, and nanotechnology.[4] Aggregation-induced emission (AIE) and aggregation-caused quenching (ACQ) are two important optical properties of luminescent materials that aim to explore luminescence or quenching at the aggregate level.[5] The two effects exhibit converse fluorescence characteristics; as the aggregation degree of molecules increases, the fluorescence intensity weakens for ACQ phores but strengthens for AIEgens. These distinct fluorescence properties of their aggregates inspire chemists to synthesize individual molecules that bind ACQ and AIE moieties, and tunable multicolour fluorescence is achieved by controlling the degree of aggregation because the π–π stacking of ACQ moieties is prevented by the twisted molecular geometry of AIE rotors in the aggregated state.[6] On the other hand, temperature, solvent effect, concentration, and solubility are factors that influence molecular aggregation.[7] Therefore, combining AIE and ACQ into a single molecule may integrate the strengths of both types of fluorophores and offer an alternative strategy for solvent discrimination. In addition, it is important to determine the correlation between basic aggregate-properties and relaxation dynamics of multiple organic dye molecular aggregates in order to design materials for electroluminescence, sensors, organic lasers, photocatalysis, and bioimaging.[8] The degree of molecular aggregation

*[a]Anhui Province Key Laboratory of Optoelectronic Material Science and Technology, School of Physics and Electronic Information, Anhui Normal University, Wuhu, 241002, China. E-mail: wgy@ahnu.edu.cn; zhoulu@ahnu.edu.cn*

*[b]Shandong Province Key Laboratory of Medical Physics and Image Processing Technology, School of Physics and Electronics, Shandong Normal University, Jinan, 250014, China. E-mail: linll@sdnu.edu.cn*

*[c]Key Laboratory of Functional Molecular Solids, Ministry of Education, College of Chemistry and Materials Science, Anhui Normal University, Wuhu, 241002, China*

† Electronic supplementary information (ESI) available. CCDC 2144544. For ESI and crystallographic data in CIF or other electronic format see DOI: https://doi.org/10.1039/d3ra06359c

always depends on various types of molecular interactions, including π–π stacking, hydrogen bonding, hydrophobic or electrostatic interactions, and van der Waals forces.[9] All of these interactions alter the photophysical behaviors. Therefore, there is an urgent need for systematic studies on the dynamics of excited states at different degrees of molecular aggregation, which will benefit the application and development of organic dye molecules in various fields.[10]

Herein, a novel fluorescent material **TPEIP** containing tetraphenylethylene (TPE) with a propeller shape and phenazine unit was designed and synthesized *via* the cyclization reaction of 2,3-diamino-phenazine with 4-tetraphenylenthenealdehyde. **TPEIP** possesses both AIE (TPE) and ACQ (phenazine) moieties. In methanol solvent, the fluorescence of **TPEIP** can be significantly quenched due to molecular aggregation and solvation effect. Therefore, the excited state dynamics of **TPEIP** aggregation in methanol, ethanol and DMSO/water mixture solutions were comprehensively investigated by femtosecond time-resolved transient absorption (TA) and computational studies to determine the relaxation dynamics of **TPEIP** molecular aggregates. Notably, the singlet state only occurred in **TPEIP** aggregates, and the intersystem crossing (ISC) rate can be tuned *via* the simple addition of water to **TPEIP** solutions in DMSO. Radiative transitions progressively decrease and eventually disappear with increasing degrees of **TPEIP** aggregation. These results not only clarify the unique excellent methanol-discriminating behavior of **TPEIP** but also provide an approach for determining the excited-state dynamics of molecular aggregates.

## Experimental section

### Synthesis of compounds TPEIP and PIP

A mixture of 2,3-diamino-phenazine (0.21 mg, 1.0 mmol), 4-(1,2,2-triphenylvinyl)benzaldehyde (1.08 g, 3 mmol), 1.0 mL acetic acid (AcOH) and *N*,*N*-dimethylformamide (DMF) were magnetically stirred and heated at 90 °C for 12 h. After cooling to room temperature, the yellow precipitate was filtrated, washed with hot absolute ethanol three times, then recrystallized with DMF-H$_2$O to get yellow powdery product **TPEIP** (0.25 g, 0.45 mmol) in 45% yield, $^1$H-NMR (DMSO-$d_6$, 400 MHz) 13.36 (s 1H, NH), 8.44 (s 1H, ArH), 8.23–8.21 (m 2H, ArH), 8.13 (d *J* = 8.36 Hz, 2H, ArH), 7.90–7.89 (m 2H, ArH), 7.24–7.13 (m 12H, ArH), 7.07–7.0 (m 6H, ArH). $^{13}$C-NMR (DMSO-$d_6$, 100 MHz) 159.25, 147.05, 142.87, 142.68, 142.02, 141.82, 140.11, 139.78, 131.57, 130.80, 130.67, 129.82, 128.97, 128.1, 127.94, 127.37, 127.02, 126.93, 126.69. ESI-MS *m/z*: calcd. for C$_{39}$H$_{26}$N$_4$, 550.22; Found, 551.22 (Scheme 1).
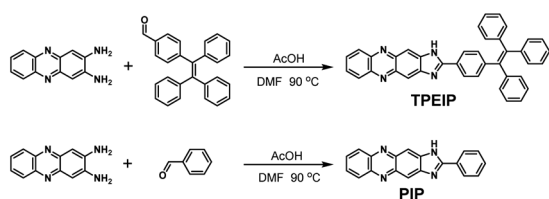
**Scheme 1** Synthesis of **TPEIP** and **PIP**.

## Results and discussion

### UV-vis absorption and fluorescence emission properties

To study the spectrum of **TPEIP** molecule in various solvents, UV-vis and fluorescence experiments were carried out in various solvents, *i.e.*, dimethyl sulfoxide (DMSO), acetonitrile (ACN), dimethylformamide (DMF), methanol (MeOH), ethanol (EtOH), acetone, tetrahydrofuran (THF), ethyl acetate (EA), dichloromethane (DCM), chloroform (CHCl$_3$), toluene (Tol). In the UV-vis absorption spectra, **TPEIP**, which contains a conjugated phenazine group, exhibited strong absorption peaks at approximately 250–320 nm and 406–413 nm in various organic solvents with solvatochromism of about 7 nm and shoulder absorptions in the range of 450–500 nm (Fig. S1†). However, the UV-vis absorption spectra of **TPEIP** did not show significant dependence on solvents because neither solvent polarity nor hydrogen bonding influenced the energy levels. Furthermore, fluorescent measurements for **TPEIP** were performed in various organic solvents ($\lambda_{ex} = 410$ nm). The photophysical properties, including the quantum yield ($\Phi_f$) and fluorescence lifetime of **TPEIP** in various organic solvents, were summarized in Table S1.† Interestingly, the fluorescence emission intensity of **TPEIP** was significantly lower in methanol and ethanol compared to other organic solvents. Specifically, in methanol solvent, the fluorescence intensity was seven times weaker than that observed in ethanol (Fig. 1a). More importantly, methanol solvents can be discriminated by the naked eye as they exhibit almost no fluorescence emissions in methanol and yellow or green fluorescence in other solvents. The specificity of **TPEIP** fluorescence emission in methanol and ethanol was investigated by performing concentration-dependent UV absorption and fluorescence spectra of **TPEIP** in both solvents (Fig. S2–S4†). The TPEIP absorption peak was found to increase in proportion with concentration, surpassing the detection limit at concentrations exceeding 0.5 mM (Fig. S2†). For concentration-dependent fluorescence spectra (Fig. S3†), the fluorescence emission intensity of **TPEIP** initially increased, but subsequently decreased and the emission peak redshifted upon increasing the concentration. The intensity reached its maximum at a concentration of 0.02 mM, indicated ACQ behavior when the concentration exceeded 0.02 mM. The strong ACQ effect may be attributed to the π–π stacking of the nearly planar phenazine unit. Conversely, when the concentration was below 0.02 mM, weak fluorescence intensity was observed due to the solvation effect on **TPEIP**. The fluorescence emission color of **TPEIP** in EtOH under 365 nm ultraviolet light was observed with the naked eye, transitioning
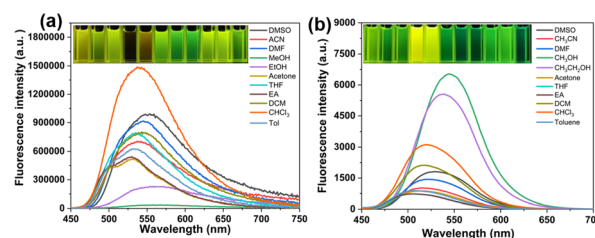
**Fig. 1** The fluorescence spectra of **TPEIP** (a) and **PIP** (b) (2 × 10$^{-5}$ mol L$^{-1}$) in various solvents.

**Paper**

from colorless to yellow and then orange. However, as the concentration of **TPEIP** in MeOH increases, the fluorescence emission color of the solution changes from colorless to yellowish to reddish (Fig. S4†).

The influence of the tetraphenyl moiety on the spectral characteristics of **TPEIP** molecular structure was further explored *via* the design and synthesis of a phenazine derivative **PIP** featuring an additional phenyl group. UV-vis and fluorescence experiments of **PIP** were also conducted in various solvents (Fig. 1 and S1†). Compared to **TPEIP**, **PIP** was more sensitive to solvent polarity in the fluorescence spectra, resulting in a redshift of the maximum fluorescence emission peak with increasing solvent polarity. In addition, the emission maxima of **PIP** in ethanol and methanol were 539 nm and 544 nm, respectively. This was accompanied by a significant enhancement in fluorescence emission, resulting in yellow fluorescence colors. It was difficult to distinguish between methanol and ethanol with the naked eye because **PIP** did not aggregate in MeOH or EtOH solvents (Fig. 1b).

To the best of our knowledge, the aggregation-caused quenching (ACQ) effect can be induced by the aggregation of phenazine groups. Thus, we have verified whether the fluorescence quenching of **TPEIP** in MeOH or EtOH was caused by molecular aggregation. The dynamic light scattering (DLS) experiment proved to be an effective method for measuring solute aggregation in solution. Dynamic light scattering experiments were conducted on **TPEIP** (0.02 mM) in various solvents, revealing significant aggregation sizes in MeOH and EtOH. However, the aggregate size of **TPEIP** in other solvents was below the instrument's limit, making it impossible to determine the aggregate size. At the same concentration (0.02 mM), the average aggregation sizes of **TPEIP** in MeOH and EtOH were 116 nm and 193 nm (Fig. S5c†), respectively. These results fully indicate that **TPEIP** forms aggregates in methanol and ethanol. The concentration-dependent DLS analysis of **TPEIP** in EtOH and MeOH was also conducted, which revealed an increase in the average size of aggregates with higher concentrations. It was worth noting that no aggregation was observed at concentrations below 6 μM. Additionally, when comparing equivalent concentrations, the degree of aggregation in ethanol exceeded that in methanol (Fig. S5†). The aggregation of molecules depends on intermolecular interactions, such as π–π stacking, hydrogen bonding, hydrophobic or electrostatic interactions, and van der Waals forces. These interactions control the extent of molecular aggregation and influence the photophysical behaviors. To gain further insight into the molecular structure in the solid state, the crystals of **TPEIP** were grown for X-ray analysis by slowly evaporating their MeOH solution. The molecular structure of **TPEIP** was shown in Fig. 2. The 1*H*-imidazo[4,5-*b*]phenazine and phenyl group units were nearly spatially parallel in the crystal. In the packing of the crystal structure, π–π stacking interactions (centroid distances of 3.392 and 3.411 Å) can be observed between the phenazine units. Additional C–H···π interactions were found between the phenyl group in adjacent TPE units, leading to the formation of a 3D structure. Due to multiple weak interactions and the large steric hindrance of the TPE moiety, **TPEIP** exhibited a head-to-
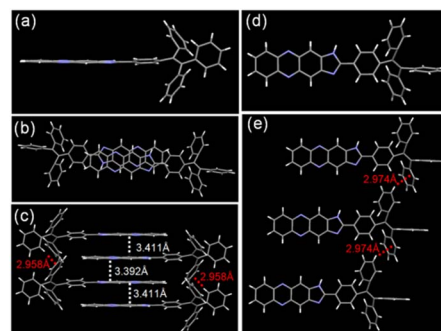


Fig. 2  **TPEIP** crystal analysis (left column). The molecular conformation in (a) side and (d) top view. The overlapping between adjacent molecules in the dimer was viewed in top view (b). Partial view of the molecular packing in side view (c). The molecular distance between adjacent molecules viewed in side view (e).

tail, antiparallel herringbone packing structure in its crystalline state, as depicted in Fig. 2c.

To further investigate the molecular ACQ effect, UV-vis and fluorescence spectra were employed to investigate the ACQ effect of **TPEIP** in DMSO/$H_2O$ mixture solutions with varying degrees of aggregation. The UV absorption of **TPEIP** decreased as the water ratio increased (Fig. S6†). In the fluorescent spectrum (Fig. S6†), the fluorescence intensity of **TPEIP** was significantly reduced with a redshift of approximately 15.0 nm when the $H_2O$ concentration was 10%. Within the range of 20–100% $H_2O$ content, the fluorescence intensity continued to decrease until it was completely quenched, indicating that molecular aggregation caused a rapid decline in emission intensity due to the ACQ effect resulting from an increase in $H_2O$ content. Based on other literature reports on similar structures, as well as the single crystal structure of **TPEIP** and the photophysical phenomena of TPEIP in methanol or ethanol. Three key factors contributed to this ACQ effect: (i) **TPEIP** was hydrophobic, DMSO and $H_2O$ act as good and poor solvents, respectively. The higher the water content, the greater degree of molecular aggregation; (ii) the crystal structure of **TPEIP** revealed a strong π–π stacking between the phenazine units, with the molecules arranged in a head-to-tail manner. This arrangement increased the distance between the two TPE units and prevented them from being closely packed. Therefore, ACQ between phenazine units was dominant in **TPEIP** aggregates; (iii) compared to other solvents, the fluorescence intensity of **TPEIP** was noticeably weaker in methanol or ethanol. In DMSO/$H_2O$ mixture solutions, $H_2O$ as a protic solvent, the fluorescence emission intensity of **TPEIP** is also weakened.

## Theoretical simulation of TPEIP monomers absorption

The absorption spectra of **TPEIP** monomers in DMSO, MeOH and EtOH were calculated using density functional theory (DFT) at the M06-2X/6-31G* level (Fig. S7†). The solvent effect was considered by using the polarizable continuum model (PCM). The calculated absorption spectra corresponded to the experimental results. There were two absorption peaks in the spectra, and the highest absorption peak was induced by the
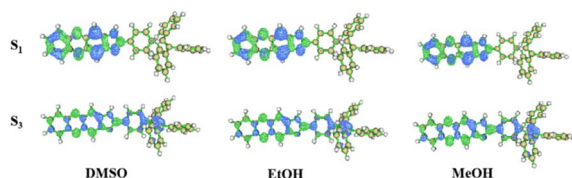
**Fig. 3** Electrons and holes distribution in $S_1$ and $S_3$ for **TPEIP**-monomers in DMSO, EtOH and MeOH (green represents the electron distribution, blue represents the hole distribution).

electron transition from the ground state ($S_0$) to the third excited singlet state ($S_3$). The transition from $S_0$ to the first singlet excited state ($S_1$) also contributes to a weak absorption peak. The absorption spectra of the **TPEIP** monomers in the three solvents were almost the same. The distributions of electrons and holes in $S_1$ and $S_3$ were plotted in Fig. 3. It was evident that for **TPEIP** in the three solvents, $S_1$ represents localized excitation (LE) states with both electrons and holes located at the $1H$-imidazo[4,5-$b$]phenazine unit. As for $S_3$, the transition exhibits a slight charge transfer (CT) property, which also involves the TPE unit.

### Theoretical confirmation of ACQ in TPEIP

To confirm that aggregation can induce fluorescence quenching in MeOH, the light emitting properties of **TPEIP** monomers in MeOH and the crystal state were theoretically studied through the PCM method and the combined quantum mechanics and molecular mechanics (QM/MM) method, respectively. In the QM/MM calculation, the ONIOM model was adopted, as show in Fig. 4a. The central molecule was calculated using the QM method at the M06-2X/6-31G level, while the remaining molecules were calculated using the MM method with the UFF force field. In Fig. 4b, we find that the oscillator strength of **TPEIP** in the crystal state was significantly smaller than that of **TPEIP** monomers in MeOH solvent, resulting in weak emission in the crystal state. From the electron distributions of the highest occupied molecular orbital (HOMO) or HOMO-2 and the lowest unoccupied molecular orbital (LUMO) that contribute most to the excitation of $S_1$, we find that the transition changes from $\pi \rightarrow \pi^*$ to n $\rightarrow \pi$; thus, a smaller oscillator strength was obtained in the crystal state. The calculated wavelength in the crystal state was 29 nm larger than that of the **TPEIP** monomers in solvent (Table S2†). The radiative rate calculated in the crystal state was approximately three orders of magnitude smaller than that in the solvent, and the non-radiative rates were almost the same in both states. Consequently, weak emission was expected for **TPEIP** in the crystal state. This result indicates that aggregation can influence the transition properties of excited states and thus affect the light-emitting properties, which corresponds with experimental results.

### Theoretical simulation of excited dynamic process

The energy diagram of TPEIP-monomer in three solvents were also plotted in Fig. 5. It was found that the energy diagram for them were quite similar. The four triplet states were lower in energy than $S_1$. It implied that triplet states might participate in
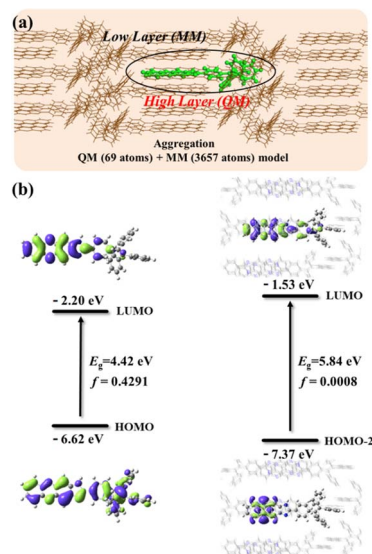


**Fig. 4** (a) ONIOM model of **TPEIP** calculated in crystal state. (b) Electron distribution of HOMO (HOMO-2) and LUMOs and their energy gaps for **TPEIP**-monomers in MeOH solvent and crystal state.

the excited states decay process. For comparison, the energy distribution of excited states for TEPIP in crystal state was also plotted in Fig. 5. It was a little different from that in solvent. In crystal state, the energy of $T_5$ was higher than that of $S_2$, while it was lower than $S_2$ in solvent. In addition, the energy gap between $S_2$ and $S_1$ was smaller than that in solvent. It was possible that the excited states could quickly decay from $S_3$ to $S_2$ and $S_1$ in crystal state, while $S_2$ could decay to $T_5$ by intersystem crossing due to the small energy gap between $S_2$ and $T_5$ as well as large energy gap between $S_2$ and $S_1$ in DMSO. Then $T_5$ will decay to $T_2$ and $T_1$, which would induce another absorption from triplet states. It was indicated that aggregation could influence the energy diagram and also the excited dynamic processes.

### Ultrafast transient absorption spectra

Transient absorption (TA) measurements can detect transition routes and transition rates between excited state energy levels of samples. To investigate **TPEIP** on the dynamics of excited states,
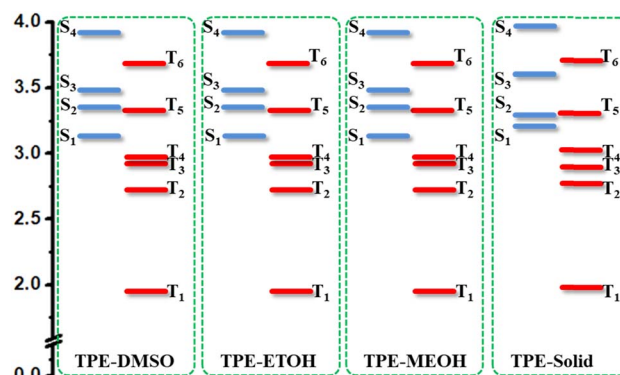


**Fig. 5** Energy diagram of excited states for **TPEIP**-monomer in DMSO, EtOH, MeOH and crystal state.

femtosecond transient absorption spectra of **TPEIP** (0.02 mM) were obtained in DMSO, MeOH and EtOH at 380 nm femtosecond pulse excitation (Fig. 6). **TPEIP** monomer exhibited a completely different TA spectrum in DMSO compared to that in methanol and ethanol. As shown in Fig. 6a, the excited state absorption (ESA) bands exhibited a slight blueshift and intensity increase due to the solvent–solute interaction (solvation). Subsequently, the ESA intensity gradually decays and accompanied by the emergence of two new ESA bands at 460 nm and 520 nm, indicating the generation of new excited states. Then, there were barely any changes in the whole TA spectra within the 7 ns detection time window. However, the initial transient absorption spectra were almost identical in MeOH and EtOH solutions, exhibiting negative ground state bleaching (GSB) in the 400–430 nm region, positive ESA across wavelengths of 440–650 nm, and no stimulated emission (SE) band. As shown in Fig. 6b, the ESA band exhibited a significant blueshift in the first 10 ps in MeOH due to solvent–solute interaction (solvation), which has also been observed in EtOH with a longer blueshift time (100 ps). These phenomena may be caused by **TPEIP** aggregates' higher degree of aggregation in MeOH than in EtOH. Afterwards, the ESA band gradually decreased and disappeared, indicating a continuous return of excited-state molecules to the ground state. Interestingly, the decay time of the **TPEIP** excited state band in EtOH was longer than that of **TPEIP** in MeOH (Fig. 6c), which was consistent with the fluorescence emission lifetime of **TPEIP** in EtOH.

Global fitting of fs-TA data was carried out to thoroughly elucidate the process of these spectral evolutions, and the time constants of the corresponding excited state processes were shown in Table 1. The target evolution models and species-associated difference spectra (SADS) were shown in Fig. 7 and S8,† while temporal concentrations of corresponding species and kinetics traces at several selected typical wavelengths were depicted in Fig. S9 and Table S3.† For the **TPEIP** monomers in DMSO, the first species-associated spectra (SADS-1) exhibit GSB signal at 413 nm and ESA signal at 540 nm, The time constant of the process associated with solvation-stabilization relaxation processes was 4.0 ps. This time scale indicates that the $S_1$ excited state undergoes solvent reorganization facilitated by conformational relaxation.[11] Subsequently, one section of the $S_1$ state (the second SAS) relaxes

**Table 1** Time constants estimated for different excited-state deactivation processes of **TPEIP**-monomers in DMSO, and **TPEIP**-aggregates in MeOH (b) and EtOH (c) solvents determined by fs-TA measurements (0.02 mM)

| Solvent | $\tau_1$ (ps) | $\tau_2$ (ps) | $\tau_3$ (ns) |
|---------|---------------|---------------|---------------|
| DMSO | $4.0 \pm 0.1$ | $966.2 \pm 2.6$ | Long-lived |
| MeOH | $7.0 \pm 0.1$ | $61.2 \pm 1.0$ | — |
| EtOH | $25.9 \pm 0.4$ | $412.2 \pm 16.0$ | — |

to the $S_0$ state, while the other section relaxes to the triplet state. Nanosecond transient absorption spectroscopy (ns-TA) was performed to characterize the triplet state under deaerated and aerobic conditions in DMSO (Fig. S10 and S11, Table S4†). The triplet lifetime of **TPEIP** monomers was twice as long under deaerated conditions (210 ns) than under aerated conditions (87.7 ns) in DMSO. This demonstrates that the triplet state was generated by **TPEIP** monomers in DMSO because oxygen could quench the triplet state. However, for **TPEIP** aggregates in MeOH and EtOH, there were only two SADS processes ($S_1^{ex}$ and $S_1^{em}$).

These phenomena suggest that aggregation inhibited intersystem crossing (ISC) (Fig. 7). The lifetimes of SADS-1 ($S_1^{ex}$) were 7 ps and 25.9 ps for **TPEIP** aggregates in MeOH and EtOH, respectively. Therefore, SADS-2 represents the geometrically relaxed $S_1$ state ($S_1^{Rlx}$), and the time constants of the radiative pathway were 61.2 and 412.2 ps ($\tau_2$) for **TPEIP** aggregates in MeOH and EtOH, respectively. Because the time constant of the radiative pathway ($S_1^{Rlx}$) was longer in EtOH, the fluorescence emission intensity of **TPEIP** aggregates was weaker in MeOH than in EtOH. It was further indicated that excited state dynamics were affected by molecular aggregation.

To investigate the effect of molecular aggregation on excited-state dynamics, the differential absorption 3D maps of transient absorption and the corresponding time evolutions of **TPEIP** in DMSO/$H_2O$ mixtures with water contents of 5%, 10%, 15%, 20%, 30%, and 40% were displayed in Fig. 8 and S12.† The TA spectral features of **TPEIP** in MeOH or EtOH were similar to those in water content exceeding 10%. Within the test time window, there was only a singlet signal, which gradually weakened with increasing water proportion. This suggests that the
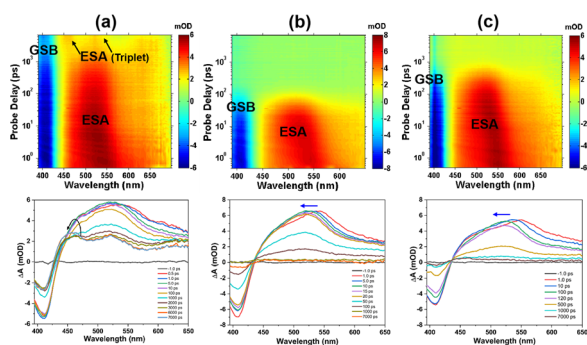


**Fig. 6** Differential absorption 3D map of the TAS data (0.02 mM) matrix after 380 nm excitation (upper row) and time evolution of the TA spectra (lower row) of **TPEIP**-monomers in DMSO (a), and **TPEIP**-aggregates in MeOH (b) and EtOH (c) solvents.
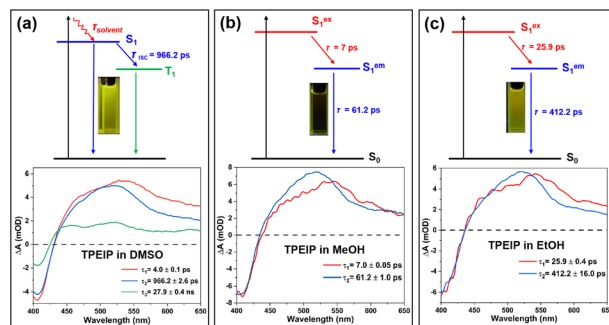


**Fig. 7** Kinetictive model used for global target analysis (upper row) and obtained species-associated difference spectra (SADS) (lower row) of **TPEIP**-monomers in DMSO (a), and **TPEIP**-aggregates in MeOH (b) and EtOH (c) solvents.
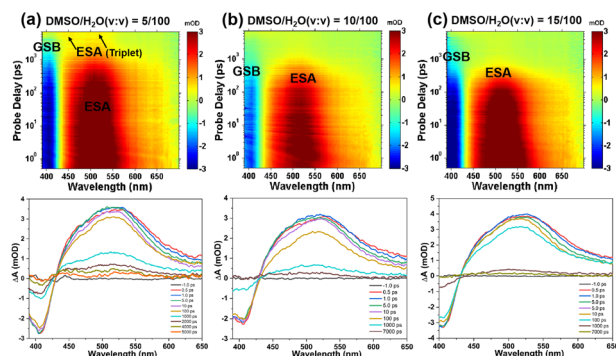
**Fig. 8** Differential absorption 3D map of the TAS data matrix after 380 nm excitation (upper row) and time evolution of the TA spectra (lower row) of **TPEIP** in DMSO/H$_2$O mixed solvents with 5% (a), 10% (b), 15% (c) of H$_2$O content.

phenyl group's geometrical constraint hindered any ISC in most of the chromophores. Specifically, the restriction of rotation was caused by the proximity of individual **TPEIP** molecules to each other. Subsequently, ISC transitions occur during relaxation from the $S_1^{Rlx}$ state to the triplet state $T_1$. The decay of $T_1$ reinstates the ground state within 11.9 ns for a water content of 5%. However, the lifetimes of the $S_1^{Rlx}$ state were 614 ps, 398.1 ps, 256.1 ps, 155.9 ps, and 122.6 ps for water contents of 10%, 15%, 20%, 30%, and 40% respectively. In this context, the triplet state $T_1$ was not generated for water contents greater than 5%, and the relaxation time of the $S_1^{Rlx}$ state becomes shorter while the signal strength weakens with increasing water content ratio. Notably, the time scales of the $S_1^{Rlx}$ state derived from single wavelength kinetics were consistent with the evolution times SADS-2, which were evaluated based on global target analysis (Fig. S15 and Tables S5, S9†). The lifetimes of the $S_1^{Rlx}$ state in DMSO/H$_2$O mixed solvents with 0%, 5%, 10%, 15%, 20%, 30% and 40% H$_2$O content at a wavelength of 462 nm were as follows: 636.5 ps, 408.9 ps, 226.1 ps, 142.5 ps and 102.9 ps (Table S5†). These arguments further confirm that the fluorescence intensity of **TPEIP** aggregates was weaker in MeOH than in EtOH due to different degrees of aggregation.

We analyze the global fitting of the 3D fs-TA data matrices to reveal individual signatures of each excited state and present the kinetic models for **TPEIP** in DMSO solutions with 5% (a), 10% (b), and 15% (c) water content, as depicted in Scheme 2. The population evolution of the corresponding SADS was
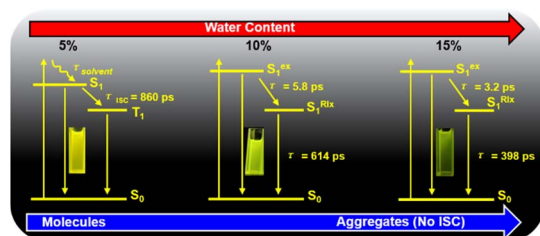
illustrated in Fig. S9.† The initially excited state ($S_1^{ex}$) lifetimes were 3.9, 5.8, 3.2, 3.3, 4.6 and 4.5 ps for 5%, 10%, 15%, 20%, 30% and 40% water content, respectively (Fig. S13 and S14†). For **TPEIP** solutions with a water content of only 5%, the geometrically relaxed $S_1$ state ($S_1^{Rlx}$) was formed *via* state deactivation ($S_1^{ex}$) caused by geometrical relaxation.

## Conclusions

In conclusion, we synthesize a novel tetraphenylethene-based phenazine-imidazole derivative (**TPEIP**) with AIE and ACQ units. **TPEIP** exhibits brilliant fluorescence in nonprotic solvents. However, **TPEIP** shows the weakest fluorescence intensity in MeOH solvent due to molecular aggregation. Different degrees of **TPEIP** aggregation resulted in a specific fluorescence response. The effects of **TPEIP** aggregation on excited states dynamics were studied in detail by TA and DFT, revealing that the rate of ISC and radiative transitions progressively decrease until they disappear with increasing degrees of **TPEIP** aggregation. This work provides an approach for understanding the excited-state dynamics of molecular aggregates.

## Author contributions

Gui-Yuan Wu: funding acquisition, project administration, resources, supervision, writing – review & editing. Hui-Min Zhu and Hao Li: formal analysis, data curation. Kai Zhang: theoretical simulation. Xianyi Zhang: project administration, supervision, writing – review & editing. Dong Yan: formal analysis, data curation. Xiu-Du Zhang: formal analysis, data curation. Lili Lin: theoretical simulation, investigation, validation. Zhou Lu: funding acquisition, supervision, writing – review & editing.

## Conflicts of interest

There are no conflicts to declare.

## Acknowledgements

## Notes and references

1  A. P. Alivisatos, P. F. Barbara, A. W. Castleman, J. Chang, D. A. Dixon, M. L. Klein, G. L. McLendon, J. S. Miller, M. A. Ratner, P. J. Rossky, S. I. Stupp and M. E. Thompson, *Adv. Mater.*, 1998, **10**, 1297; Y. Tu, Z. Zhao, J. W. Y. Lam and B. Z. Tang, *Matter*, 2021, **4**, 338–349.

2  P. W. Anderson, *Science*, 1972, **177**, 393; B. Liu and B. Z. Tang, *Angew. Chem., Int. Ed.*, 2020, **59**, 9788.



**Scheme 2** Excited state relaxation of **TPEIP** with increasing degrees of aggregation.

3 J. Mei, N. L. C. Leung, R. T. K. Kwok, J. W. Y. Lam and B. Z. Tang, *Chem. Rev.*, 2015, **115**, 11718; Z. Zhao, W. He and B. Z. Tang, *Acc. Mater. Res.*, 2021, **2**, 1251; H. Yao, *Annu. Rep. Prog. Chem., Sect. C*, 2004, **100**, 99; Y. Shi, S. Wang, W. Tao, J. Guo, S. Xie, Y. Ding, G. Xu, C. Chen, X. Sun, Z. Zhang, Z. He, P. Wei and B. Z. Tang, *Nat. Commun.*, 2022, **13**, 1882.

4 Y. Wang, J. Nie, W. Fang, L. Yang, Q. Hu, Z. Wang, J. Sun and B. Z. Tang, *Chem. Rev.*, 2020, **120**, 4534; L.-J. Chen and H.-B. Yang, *Acc. Chem. Res.*, 2018, **51**, 2699; X. Sun, W. Huang, Y. Zhou and D. Yan, *Phys. Chem. Chem. Phys.*, 2010, **12**, 11948; J. Li, Y. Liu, Y. Qian, L. Li, L. Xie, J. Shang, T. Yu, M. Yi and W. Huang, *Phys. Chem. Chem. Phys.*, 2013, **15**, 12694; K. Li, S. Li, L. Liu, W. Huang, Y. Wang, C. Yu and Y. Zhou, *Phys. Chem. Chem. Phys.*, 2019, **21**, 19995.

5 W. J. Li, X. Q. Wang, D. Y. Zhang, Y. X. Hu, W. T Xu, L. Xu, W. Wang and H. B. Yang, *Angew. Chem., Int. Ed.*, 2021, **60**, 18761.

6 Q. Wan, B. Zhang, J. Tong, Y. Li, H. Wu, H. Zhang, Z. Wang, Y. Pan and B. Z. Tang, *Phys. Chem. Chem. Phys.*, 2019, **21**, 9837; B. S. Shivaji, R. Boddula and S. P. Singh, *Phys. Chem. Chem. Phys.*, 2022, **24**, 15110; Y. Zhang, B. He, J. Liu, S. Hu, L. Pan, Z. Zhao and B. Z. Tang, *Phys. Chem. Chem. Phys.*, 2018, **20**, 9922; G. Yakalı, *Phys. Chem. Chem. Phys.*, 2021, **23**, 11388; H. Wei, Y. Zeng, Q. Li and X. Zheng, *Phys. Chem. Chem. Phys.*, 2022, **24**, 25487; B. Yu, D. Liu, Y. Wang, T. Zhang, Y.-M. Zhang, M. Li and X.-A. Zhang, *Phys. Chem. Chem. Phys.*, 2018, **20**, 23851.

7 M. Son, K. H. Park, C. Shao, F. Würthner and D. Kim, *J. Phys. Chem. Lett.*, 2014, **5**, 3601; K. Dirian, S. Bauroth, A. Roth, Z. Syrgiannis, F. Rigodanza, M. Burian, H. Amenitsch, D. I. Sharapa, M. Prato, T. Clark and D. M. Guldi, *Nanoscale*, 2018, **10**, 2317.

8 J. Guo and H. X. Zhou, *Chem. Rev.*, 2016, **116**, 6503; T. R. Nelson, A. J. White, J. A. Bjorgaard, A. E. Sifain, Y. Zhang, B. Nebgen, S. Fernandez-Alberti, D. Mozyrsky, A. E. Roitberg and S. Tretiak, *Chem. Rev.*, 2020, **120**, 2215; M. Lv, X. Lu, Y. Jiang, M. E. Sandoval-Salinas, D. Casanova, H. Sun, Z. Sun, J. Xu, Y. Yang and J. Chen, Near-Unity Triplet Generation Promoted via Spiro-Conjugation, *Angew. Chem., Int. Ed.*, 2022, **61**, e202113190; I. A. Heisler and S. R. Meech, *Chem. Soc. Rev.*, 2021, **50**, 11486; X. Luo, J. Li, J. Zhao, L. Gu, X. Qian and Y. Yang, *Chin. Chem. Lett.*, 2019, **30**, 839; P.-P. Jia, L. Xu, Y.-X. Hu, W.-J. Li, X.-Q. Wang, Q.-H. Ling, X. Shi, G.-Q. Yin, X. Li, H. Sun, Y. Jiang and H.-B. Yang, *J. Am. Chem. Soc.*, 2021, **143**, 399; Q. Lin, X. W. Guan, S.-S. Song, H.-Y. Fan, H. Yao, Y. M. Zhang and T.-B. Wei, *Polym. Chem.*, 2019, **10**, 253.

9 H. B. Cheng, Y. Li, B. Z. Tang and J. Yoon, *Chem. Soc. Rev.*, 2020, **49**, 21; S. Liu, G. Feng, B. Z. Tang and B. Liu, *Chem. Sci.*, 2021, **12**, 6488.

10 M. W. Mara, B. T. Phelan, Z. L. Xie, T. W. Kim, D. J. Hsu, X. Liu, A. J. S. Valentine, P. Kim, X. Li, S. i. Adachi, T. Katayama, K. L. Mulfort and L. X. Chen, *Chem. Sci.*, 2022, **13**, 1715; M. Zalibera, F. Ziegs, S. Schiemenz, V. Dubrovin, W. Lubitz, A. Savitsky, S. H. M. Deng, X. B. Wang, S. M. Avdoshenko and A. A. Popov, *Chem. Sci.*, 2021, **12**, 7818; S. Cekli, R. W. Winkel, E. Alarousu, O. F. Mohammed and K. S. Schanze, *Chem. Sci.*, 2016, **7**, 3621.

11 S. V. Kirner, C. Henkel, D. M. Guldi, J. D. M. Jr. and D. I. Schuster, *Chem. Sci.*, 2015, **6**, 7293; Y. Rout, C. Montanari, E. Pasciucco, R. Misra and B. Carlotti, *J. Am. Chem. Soc.*, 2021, **143**, 9933; E. Sebastian and M. Hariharan, *J. Am. Chem. Soc.*, 2021, **143**, 13769; L. Wimberger, S. K. K. Prasad, M. D. Peeks, J. Andréasson, T. W. Schmidt and J. E. Beves, *J. Am. Chem. Soc.*, 2021, **143**, 20758.